

# Inference of geometrical analogy between magnetic domain alignment in fabricated ferromagnets and fluid flow

C. Y. TAY

*IRC in Materials for High Performance Applications, University of Birmingham, P. O. Box 363, Birmingham B15 2TT, UK*

A useful classification of fabricated ferromagnet sets can be inferred from graphs plotted with the  $H_{cB}/B_r$  and  $H_{cI}/B_r$  ratios of individual magnets which are closely similar in material composition, properties and fabrication history. For each defined set, a mean characteristic curve is obtained which may be regression fitted by (i) a logarithmic and (ii) a second-order polynomial expression. Both these regression analyses are here further discussed with the resulting suggestion that the limiting type 1 and type 2 classification of ferromagnet sets can be associated with two modes of magnetization in which the corresponding domain patterns recall, respectively, the laminar and turbulent flow patterns of a fluid system analogue.

## 1. Introduction

A few discrete quantities that are associated with the demagnetization quadrant of the hysteresis loop, such as the remanence,  $B_r$ , and the two coercivities,  $H_{cI}$  and  $H_{cB}$ , are conventionally defined to characterize the demagnetization behaviour of individual magnets. For high-coercivity rare-earth based magnets, however, this characterization is especially incomplete because their fabrication involves some powder metallurgical stages. There will be significant process-related variables which tend to influence and complicate the demagnetization characteristics of such magnets. Consequently, the difficulties of elucidating the quasi-continuous demagnetization quadrant as sampled by a limited number of discrete point parameters are accentuated. An alternative approach has been suggested [1, 2] in which the ratios of parameters, for example,  $H_{cI}/B_r$  ( $= X$ ) and  $H_{cB}/B_r$  ( $= Y$ ), are employed as the basic variables rather than the  $B_r$ ,  $H_{cI}$  and  $H_{cB}$  values themselves. For convenience, c.g.s. units are used so that  $X$  and  $Y$  are dimensionless. When the  $(X, Y)$  coordinates of similar magnets are plotted graphically, a statistical mean curve is discernible. In the present paper we extend previous logarithmic as well as second-order polynomial regression analyses relating to such  $Y$  versus  $X$  curves [1–4] in order to clarify their usefulness for specifying the magnets which define the particular sets. In the process, we suggest that the  $Y$  versus  $X$  curves are observed because the  $X, Y$  ratios can provide sufficient information about the geometry of the individual demagnetization quadrants to enable an identification of features that are common to the magnets and hence the reason for treating them as forming a particular set. At the same time the suggestion is made that the previous classification of magnet sets into types 1 and 2, may on

a more subtle level imply, instead, two corresponding modes of magnetic domain alignments. These modes are distinct in an analogous way that laminar and turbulent flow regimes may be distinguished for a fluid flow system. For magnet sets as with fluid flow, there are transitional regimes in which the magnet sets have features that are intermediate between those of types 1 and 2. These we have previously assigned to a separate type T [3–5].

Experimental data for 18 sets of fabricated magnets have previously been regression fitted to logarithmic equations of the form  $Y = KX^L$  [5]. Of this number, we have also fitted 14 sets with regression polynomial equations of the form,  $Y = \alpha + \beta X(1 - \gamma X)$  [4]. Both regression schemes have been found to give similarly good fits to the 14 sets to which they have been applied in common [4]. The original references should be consulted for further details of these 14 sets which we shall specify here with the same convenient labels as in [5]: the cold polymer-bonded  $\text{SmCo}_{x\sim 5}$  sets M(F), HD(F), M(A) and HD(A) [1–5]; and the following sintered sets, NdDyFeB [6], Neomax 30-H and 35 [7],  $\text{SmCo}_{x\sim 5}$  [8], MM-(Co, Cu, Fe, Mg) (A) and (B) (where MM = mischmetalle) [9], CoMMSm [10], CoSm [11] and the two PrSmCo sets (A) and (C) [12].

## 2. Logarithmic regression analysis

In the present paper we shall mainly discuss the four magnet sets that had previously been classed as type 2 on the basis that  $K + L \approx 1$ . Data points together with the graphs corresponding to both forms of regression equations for these sets are shown in Figs 1–4. Examples of other sets which have been classified [3] as transitional (types 2-T and T) between types 1 and 2 will only be discussed when it is required to

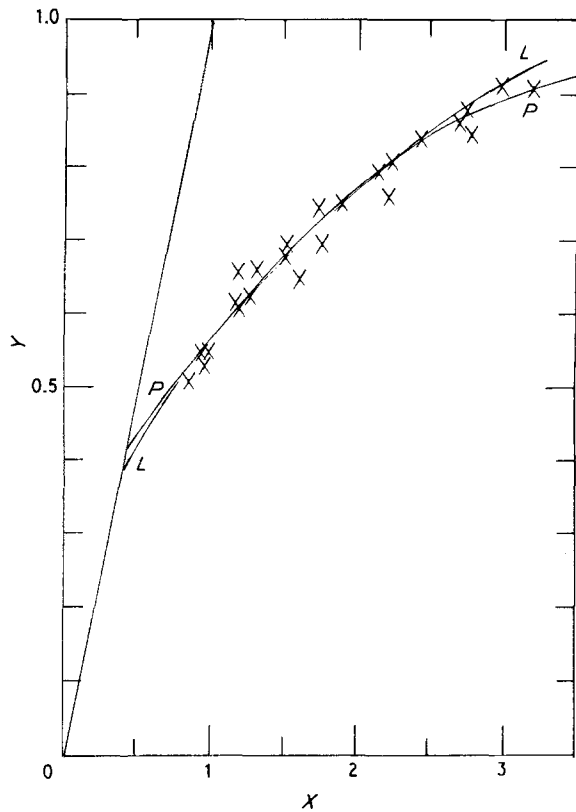


Figure 1 Empirical  $(X, Y)$  data points for the polymer bonded M(F) set together with the logarithmic (L) and second-order polynomial (P) regression-fitted curves [1-4].

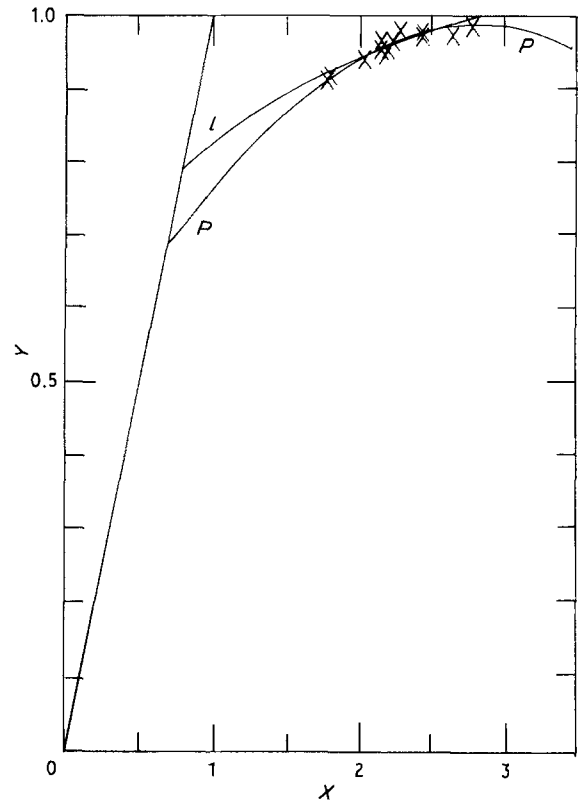


Figure 3 Empirical  $(X, Y)$  data points for the sintered PrSmCo(A) set [12] together with the logarithmic (L) and second-order polynomial (P) regression-fitted curves [1-4].

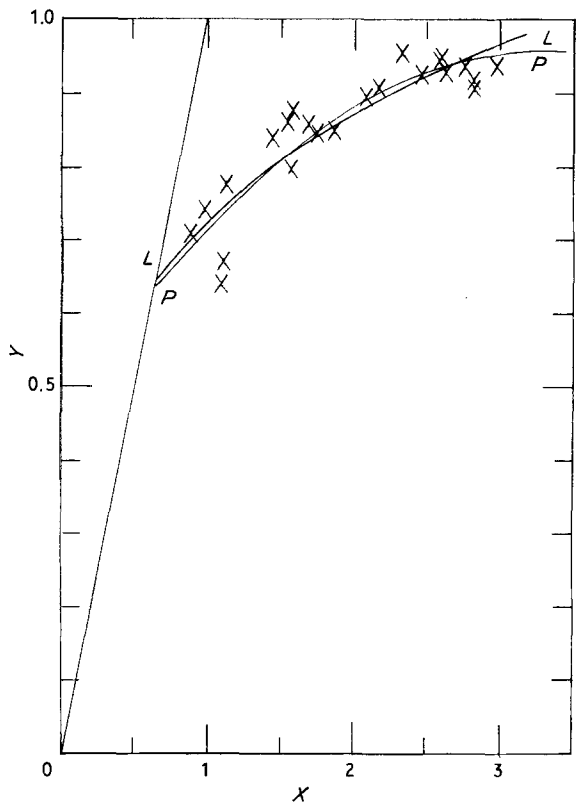


Figure 2 Empirical  $(X, Y)$  data points for the polymer bonded HD(F) set together with the logarithmic (L) and second-order polynomial (P) regression-fitted curves [1-4].

illustrate that such sets can also be regarded as the results of mixed type 1 and 2 component characteristics. Further features of the logarithmic regression analysis will now be discussed while the polynomial

analysis will be separately discussed in Section 3 below.

### 2.1. Classification of ferromagnets (I)

The equation  $Y = KX^L$  that can be fitted to the demagnetization data of a particular magnet set, where  $K$  and  $L$  are constants of fit, may also be considered as the solution of a recursion equation  $Y(n+1) = XY(n)$ , where  $n = 0, 1, 2, \dots$ , and with  $X$  at any acceptable value, so that  $Y \leq 1$  only [13]. The particular initial expression  $Y_0 = KX^L$  refers to the different magnets within a set, each with its specific  $X$  value, while the equation  $Y(n+1) = XY(n)$  generates the alternatives of a particular magnet within the set which are related to it by the recursion operation, the connotations of which are discussed below. It can be easily verified that the general solution to the recursion equation is  $Y_N = KX^{N+L}$ , where  $N = 0, 1, 2, \dots$ , with  $Y_0 = KX^L$ , that is, a formulation chosen to be identical to the regression expression as obtained from empirical data. For convenience we shall hence revert to dropping the subscript zero when referring to the initial  $N = 0$  expression which corresponds to the empirical regression equation of a particular magnet set. This chosen formulation of the general and the particular solutions to the recursion equation and indeed the equation itself is determined by the physical limitations on relations between  $Y$  and  $X$ .

#### 2.1.1. Ideal types of ferromagnets (I)

In order to discuss the chosen formulation of the logarithmic regression analysis and its suitability for

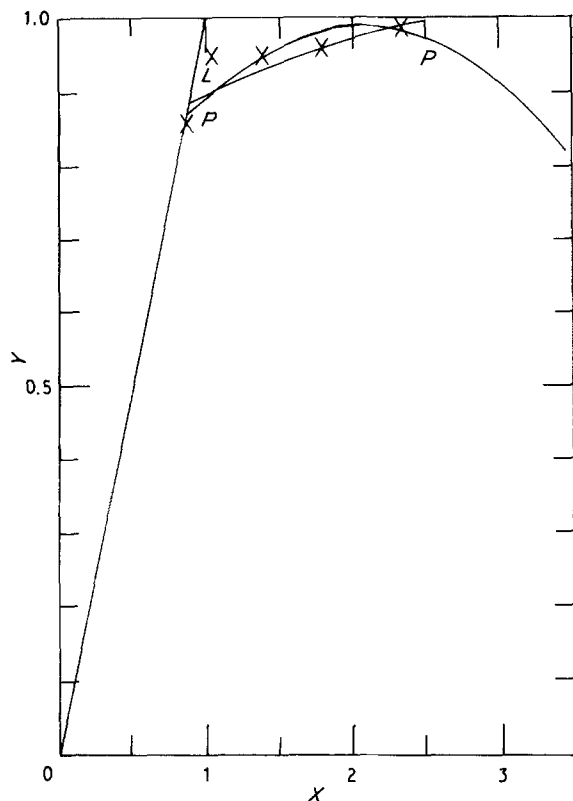


Figure 4 Empirical  $(X, Y)$  data points for the sintered NdDyFeB set [6] together with the logarithmic ( $L$ ) and second-order polynomial ( $P$ ) regression-fitted curves [1-4].

elucidating empirical data of fabricated magnet sets, we discuss firstly the limiting types of ferromagnets which possess ideally square demagnetization loops. These have been designated as ideal (or limiting) types 1 and 2, defined through the original Becker conditions [1, 2, 14]. In terms of our scaled parameters, the equations for these type 1 and type 2 ideal sets are, respectively,  $Y = X$  and  $Y = 1$ . For each of these ideal types there is a further condition on the range of applicable  $X$  values, whereby for type 1 the range is  $0 \leq X \leq 1$  and for type 2,  $X \geq 1$ , with the higher bound not clearly defined in this logarithmic equation case. Both limiting types can be represented by  $Y_0$  initial recursion expressions. To achieve this for type 1 we set  $K = 1$  and  $L = 1$  and for type 2,  $K = 1$  and  $L = 0$ . Under such a scheme, we observe that the  $Y_1$  recursion in the type 2 case for which  $X \geq 1$  maps into an extrapolation of the  $Y_0$  expression for type 1, for which  $Y$  is, however, unacceptably greater than unity except at the singular  $X = 1$  point. The  $Y_1$  expression for type 2 is thus identical to the  $Y_0$  expression for type 1 but only the latter is physically acceptable because the  $X$  range has been defined as  $0 \leq X \leq 1$ . There is no provision for a mapping of either ideal type characteristics ( $L = 0$  or  $1$ ) into the observed characteristics ( $0 < L < 1$ ) of any fabricated magnet sets.

### 2.1.2. Fabricated types of ferromagnets (I)

In order for the observed characteristics of fabricated ferromagnet sets to be accommodated in the logarithmic recursion scheme we merely require that each of the  $L$  parameter for such sets lie between the extremes

of the ideal types, that is,  $0 < L < 1$ . Except for this difference, recursion of the equation for a fabricated set may be regarded in similar terms as for the limiting types.

Principally, recursion of a mainly type 2 set equation results in acceptable  $Y \leq 1$  values only for a lower range of  $X$  values. We interpret this consequence of recursion as an emphasis of the potential type 1 component that may be present, but only for a limited range of  $X$  beyond  $X = 1$  in the original, mainly type 2 set. To illustrate this, Figs 5 and 6 show the  $Y_0$ ,  $Y_1$  and  $Y_2$  curves together with the empirical data points, for a type 2 set (the M(F) set) and a type T set (the sintered SmCo<sub>5</sub> set [81]), respectively. These graphs show that data points are present which are closer to the  $Y_1$  and  $Y_2$  curves (for  $X$  values slightly greater than unity) than the corresponding  $Y_0$  curve for the type T set but not for the type 2 set. This feature is consistent with the classification of the sets, with the type 2 set essentially entirely devoid of type 1 characteristics for  $X \approx 1$ , whereas the type T set can then include a strong admixture of type 1 characteristics.

### 2.2. Aspects of $(X, Y)$ and $(-\ln K, L)$ correspondence

When the  $Y = KX^L$  regression analysis was initially applied to sets of empirical data, the attribution of type 2 classification to four of the data sets was based on the immediately obvious observation that  $K + L \approx 1$  [1-3]. This observation is summarized in Table I by the  $K, L$  values obtained for the four type 2 sets that have been so identified. This assignment of

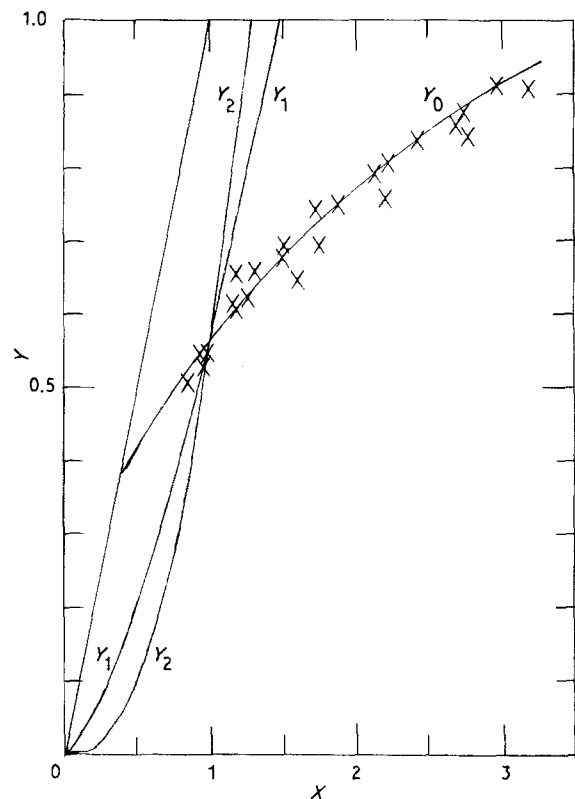


Figure 5 Empirical  $(X, Y)$  data points for the polymer bonded M(F) set together with the recursion curves ( $Y_1$  and  $Y_2$ ) of the regression fitted logarithmic curve ( $Y_0$ ).

TABLE I Empirical values of  $K$  and  $L$ , for the fitted geometrical regression equation  $Y = KX^L$ , for the four identified type 2 sets, together with  $Y$  values calculated from the equation  $Y = K(4.3471)^L$  for comparison with type 2 graphs concurrently at (4.3471, 1.0695)

Ferromagnet set	Reference	$K$	$L$	$Y = X$	$Y$ calc.
M(F)	[1-3, 5]	0.567	0.432	0.368	1.0698
HD(F)	[1-3, 5]	0.727	0.259	0.650	1.0637
PrSmCo(A)	[12]	0.828	0.182	0.794	1.0819
NdDyFeB	[6]	0.895	0.117	0.882	1.0629

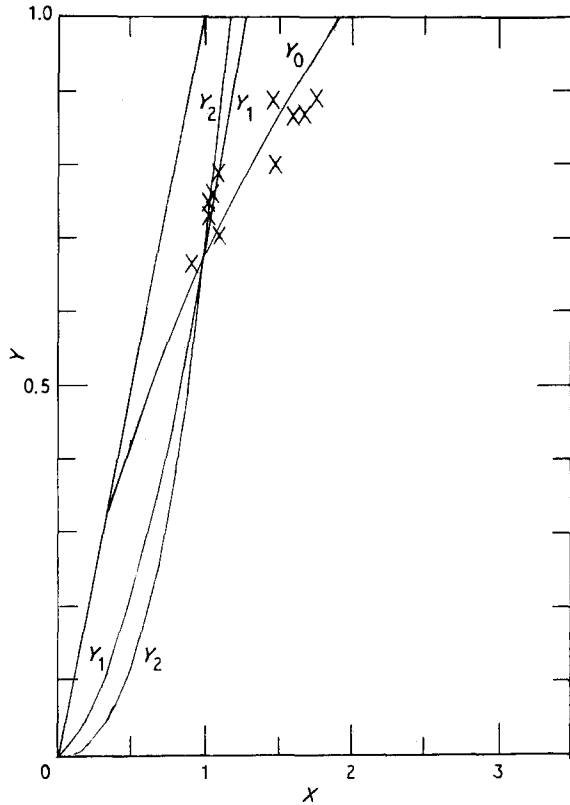


Figure 6 Empirical  $(X, Y)$  data points for the sintered  $\text{SmCo}_{x-5}$  [8] set together with the recursion curves ( $Y_1$  and  $Y_2$ ) of the regression fitted logarithmic curve ( $Y_0$ ).

type classification is consistent with the limiting type 2 set for which  $Y = 1$ , that is,  $K = 1$  and  $L = 0$ . Hence the  $K, L$  parameters of a particular set can be related to the aspects of demagnetization behaviour that are common to the individual magnets of the set. However, we shall show that the expression suggesting this relationship is actually subtly different from the simple form of  $K + L = 1$ .

Instead of examining further the original  $Y = KX^L$  form of equation we consider its logarithmic form, which transforms into the linear equation  $L = (\ln X)^{-1} [-\ln K + \ln Y]$ . When the  $(-\ln K, L)$  coordinates of the four type 2 sets are plotted (Fig. 7), we note that they are essentially collinear. The equation of this common line for the type 2 sets is  $L = 0.6805(-\ln K) + 0.0457$ . Collinearity in  $(-\ln K, L)$  coordinates corresponds to the concurrency of the original  $Y = KX^L$  curves, with the common  $(X, Y)$  point at (4.3471, 1.0695).

This  $(-\ln K, L)$  collinearity is shown numerically in Table I by values of  $Y$  calculated using the empirical  $K$  and  $L$  values in the linear  $(-\ln K, L)$  equation. This common line is also plotted in Fig. 7, together

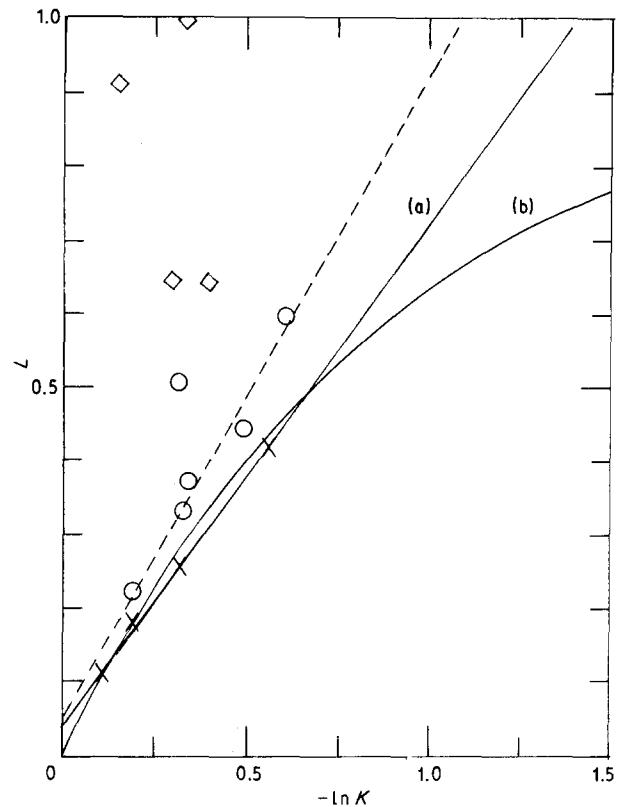


Figure 7 Parameters of logarithmic regression equations ( $Y = KX^L$ ) plotted as  $(-\ln K, L)$  coordinates for the 14 fabricated ferromagnet sets [1-4], classified as  $(\times)$  types 2,  $(\circ)$  2-T/T-2 and  $(\diamond)$  T, together with the linear equation (line a,  $L = 0.6805(-\ln K) + 0.0457$ ), and the numerical relation (curve b,  $K + L = 1$ ) as possible alternative conditions for the type 2 sets classification.

with the curve that represents the condition  $K + L = 1$ . This figure illustrates graphically the nature of the near coincidence between the more exact condition common to fabricated magnet sets with type 2 character as expressed by the collinearity of  $(-\ln K, L)$  in comparison to the numerically more immediately apparent condition of  $K + L = 1$ . There are clearly many other aspects of geometrical correspondence that exist between the  $(X, Y)$  and  $(-\ln K, L)$  representations in the logarithmic analysis. However, these are not germane to this paper and hence their further consideration is deferred for the present. Similarly, we shall not discuss here the features in Fig. 7 which are associated with the  $K, L$  parameters of the remaining 10 magnet sets.

### 3. Polynomial regression analysis

The physical necessity for  $Y \leq 1$  cannot be satisfactorily described by the general logarithmic equa-

tion,  $Y = KX^L$ . However, the range of empirical data available for our analysis is limited such that there is no definite indication of the trend of  $Y$  as a function of  $X$  as  $Y$  approaches sufficiently near to unity. As stated previously [4], type 2 magnets are necessarily fabricated through powder metallurgical process stages so that in the reconstitution of the assembly of magnetically aligned domain particles to reform the integral magnet we anticipate statistically complex inter-domain interactions to govern the eventual degree and nature of magnetic alignment that can be achieved. The principal result of such interactions, as apparently indicated by the data sets we have analysed, is the practical limitation of  $Y$  values. With higher  $X$  values there is either an asymptotic approach of  $Y$  to unity or  $Y$  reaches a peak value for the particular magnet set and then decreases again for potentially higher values of  $X$ . It is understandable that there is little practical inducement to pursue the fabrication of any magnet set beyond the stage of magnets with near peak ( $X, Y$ ) characteristics, nor to report such data were they to have been obtained. We have therefore reanalysed the same data sets with the alternative second-order polynomial which allows extrapolation to higher  $X$  values and can describe the general situation of a single  $Y$  versus  $X$  peak [4]. Application of this polynomial equation to the classification of ferromagnet sets will be briefly set out in the next subsection. Following this we discuss the scaling of  $X$ , and translation of  $Y$ , to recast the equation into a form which has been extensively employed in the formulation of the fundamental characteristics of non-linear systems behaviour [13].

### 3.1. Classification of ferromagnets (II)

An advantage of the polynomial equation over the logarithmic equation is that the regression parameters represent, respectively, the proportions of  $Y$  which are constant ( $\alpha$ ), linear ( $\beta$ ), and parabolic non-linear ( $\beta\gamma$ ) functions of  $X$ . These proportions can then be em-

ployed directly to classify the different type categories to which the empirical data sets may be assigned.

#### 3.1.1. Ideal types of ferromagnets (II)

For the type 1 ideal ferromagnet set,  $Y = X$ , purely a linear function of  $X$ . Hence, the regression parameters are  $\alpha = 0$ ,  $\beta = 1$  and  $\beta\gamma = 0$ . The type 2 ideal set equation is  $Y = 1$ , independent of  $X$ . The polynomial equation then reduces to the ideal set form where  $\alpha = 1$ , and  $\beta = 0$  and  $\beta\gamma = 0$ . Both the ideal sets are marked by the absence of any non-linear,  $\beta\gamma$ , component. For an ideal type 1 set, the only term in  $X$  is linear, with  $\beta = 1$  while the ideal type 2 set has only a constant unit value of  $Y$ . This is consistent with the above logarithmic regression view that  $K = 1$  for both ideal types but  $L$  can only be 1 ( $Y = X$ , type 1) or 0 ( $Y = 1$ , type 2).

#### 3.1.2. Fabricated types of ferromagnets (II)

Values of the polynomial regression parameters for all 14 sets of empirical data analysed are summarised in Table II. From this table we can find parallels that correspond with the scheme for the classification of ferromagnet sets according to the basis of the corresponding  $K$  and  $L$  logarithmic regression parameters. In particular, the type 2 sets have  $\alpha$  values that are higher than those obtained for the other sets that had been previously classified as types 2-T and T [3]. Correspondingly, type 2 sets also possess lower  $\beta$  values. Fabricated type 2 sets have a higher proportion of the ideal type 2 characteristics for which  $Y = \alpha = 1$ , independent of  $X$ ; simultaneously, the proportion of ideal type 1 characteristic of  $Y = \beta X = X$ , is relatively lower than for sets of types 2-T and T. The non-linear  $X$  component of  $Y$ , referred to the  $\alpha$  component (that is  $\beta\gamma/\alpha$ ) is also comparatively lower for the type 2 sets.

TABLE II Values of  $\alpha$ ,  $\beta$  and  $\beta\gamma$ , for the second-order polynomial regression equation  $Y = \alpha + \beta X - \beta\gamma X^2$ , together with the peak related values,  $\Lambda/4$  ( $= \beta/4\gamma$ )

Ferromagnet set	Reference	$\alpha$	$\beta$	$\beta\gamma$	$\Lambda/4$
Type 2					
M(F)	[1-4]	0.2852	0.3202	0.0392	0.6545
HD(F)	[1-4]	0.4537	0.3054	0.0463	0.5033
PrSmCo(A)	[12]	0.4535	0.3798	0.0682	0.5290
NdDyFeB	[6]	0.6238	0.3570	0.0874	0.3646
Type 2-T					
M(A)	[1-4]	0.1872	0.4332	0.0593	0.7905
HD(A)	[1-4]	0.1961	0.6694	0.1532	0.7314
CoSm	[11]	0.1123	0.8902	0.2372	0.8351
CoMMSm	[10]	0.2342	0.4639	0.0828	0.6497
MM-(Co, Cu, Fe, Mg) (B)	[9]	0.2738	0.5777	0.1254	0.6656
MM-(Co, Cu, Fe, Mg) (A)	[9]	0.1188	0.8157	0.2023	0.8223
Type T					
SmCo <sub>x-5</sub>	[8]	0.0919	0.8627	0.2347	0.7926
Neomax 30-H	[7]	-0.0623	1.3537	0.4370	1.0484
PrSmCo(C)	[12]	-3.5057	6.7830	2.5972	4.4287
Neomax 35	[7]	-0.0970	1.4712	0.5223	1.0361

### 3.2. Scaling of $X$ and translation of $Y$

Regression polynomial equations for all the magnet data sets have hitherto been discussed in terms of the general form  $Y = \alpha + \beta X(1 - \gamma X)$ , for which, the domain of  $X$  is  $0 \leq X \leq 1/\gamma$ . Fabricated type 2 magnets are especially distinguished by high coercivities so that the extent of the  $X$  domain can then greatly exceed the range of  $Y$  values, for which, the physical range is necessarily restricted to  $0 \leq Y \leq 1$ . This general form of polynomial equation is, therefore, not suitable for consideration as a recursion equation in  $Y$ . It can, however, be rewritten in the two alternative forms of (i)  $Y = \alpha + \Lambda X_S(1 - X_S)$  and (ii)  $Y_T = \Lambda X_S(1 - X_S)$ , where  $\Lambda = \beta/\gamma$  ( $\gamma \neq 0$  in practice),  $X_S = \gamma X$  and  $Y_T = Y - \alpha$ . In these forms,  $X$  is scaled down to  $X_S$  and  $Y$  is translated to  $Y_T$ . With the domain of  $X_S$  restricted to  $0 \leq X_S \leq 1$ , either equation can then be regarded as a suitable recursion equation in  $Y$  only, the choice depending upon the value of the particular translation term (i.e. the constant  $\alpha$ ). The recursion equations can be reformulated according as  $Y_{N+1} = \alpha + Y_{T,N+1} = \alpha + \Lambda Y_N(1 - Y_N)$ , where  $Y_N$  becomes the independent recursion variable replacing  $X_S (= \gamma X)$ . The recursion ranges are then  $\alpha \leq Y \leq \alpha + \Lambda/4$  or  $0 \leq Y_T \leq \Lambda/4$ . Both of these ranges, for 11 of the 14 ferromagnet sets we have analysed (Table II), are contained within the  $X_S$  domain of  $0 \leq X_S \leq 1$ . For the three exceptions, the  $\alpha$  values are negative so that only the  $Y_{N+1} = \alpha + \Lambda Y_N(1 - Y_N)$  recursion equation is suitable to ensure that the peak  $Y_{N+1}$  value does not exceed unity. We have also noted above that the direct use of  $X$  as the independent recursion variable in the logarithmic regression equation cannot be suitable for generating  $Y_{N+1}$  from  $Y_N$ . Because we have defined  $Y = H_{cB}/B_r$  and  $X = H_{cI}/B_r$ , the inference here that  $Y$  is the first reiterate of  $X$  which has been scaled down by the parameter,  $\gamma$ , may be taken to imply that the  $H_{cB}$  value for the demagnetization curve of a particular magnet is related to a specific fraction of the corresponding  $H_{cI}$  value; the fraction is  $\gamma$ , which is a characteristic regression parameter of the set of which that magnet is a member.

The consequences that can arise from reiteration according to the recursion equation,  $Y_{N+1} = \Lambda Y_N(1 - Y_N)$ , are very thoroughly analysed in the celebrated paper by May [15]. Different regimes of  $Y$  recursion behaviour ranging from simple, fixed points through complicated period doubling cascades to chaotically aperiodic series, can arise depending on the magnitude of the key parameter,  $\Lambda$ . We shall not need to repeat discussion of these detailed consequences in the present paper. Instead, we discuss briefly the variant form of regression equation (in  $(X_S, Y_T)$  coordinates) that is specifically more appropriate to the fabricated ferromagnet sets. The role of  $\alpha$  then is principally to ensure that the reiterated values,  $Y_{N+1}$ , keep within the physically permitted range of  $0 \leq Y \leq 1$ , even when the corresponding value of  $\Lambda$  is such that  $\Lambda Y_N(1 - Y_N)$  can, of itself, exceed this range. This observation may be surmised from the peak recursion values,  $\Lambda/4$ , which are summarized in Table II, from which we see that the  $\alpha$  values decrease monotonically from type 2 to type T ferromagnet sets, to the extent that negative

values are obtained for three of the four sets assigned as type T.

## 4. Magnetic alignment in fabricated magnet sets

The fabrication route of rare-earth (RE) high-coercivity magnets, which are classed as type 2, generally includes powder metallurgical process stages. This contrasts with type 1 magnets which have limited coercivities and can directly be magnetized in the net bulk form. Hence, the elucidation of the demagnetization characteristics of type 2 magnets will be more complicated due to the need to explain the consequences of the powder metallurgical process stages as well as the purely magnetic material characteristics which predominate in the case of type 1 ferromagnets. A major complication is that the magnetic alignment stage for a type 2 magnet is performed on an assembly of fine (micrometre) powder particles before subsequent compaction and bonding operations. A recent review (Kumar [16]) of the properties of RETM<sub>5</sub> and RE<sub>2</sub>TM<sub>17</sub> ferromagnets (TM = transition metal) comprehensively discusses both the basic material as well as fabrication process aspects that are representative of these basically type 2 magnets, and provides the background to the following discussions in the present paper.

### 4.1. $B_r$ , $H_{cI}$ and $H_{cB}$

The characteristics of the demagnetization quadrant in the hysteresis loop of a particular magnet are summarized numerically in terms of a few specific empirically measured quantities such as  $B_r$ ,  $H_{cI}$  and  $H_{cB}$ . Elucidation of the demagnetization behaviour then usually proceeds via attempts to derive each of these quantities separately as a function of several identified independent parameters which are intrinsic to the particular material and the fabrication process stages and conditions. Formally, this is expressed as  $B_r = B_r(a,b,c\dots)$ ,  $H_{cI} = H_{cI}(a,b,c\dots)$  and  $H_{cB} = H_{cB}(a,b,c\dots)$ , where  $a, b, c\dots$  refer to each of the independent parameters in the functional expressions for  $B_r$ ,  $H_{cI}$  and  $H_{cB}$ . Although not stated explicitly here, the full functional arguments will probably be far more complex, containing also non-linear terms so that the effects of an individual parameter cannot strictly be considered in isolation. A similar problem exists practically where it will be impossible to prepare magnets so that they are different in just one intrinsic parameter. Hence the dilemma that a tractable theoretical analysis will require so much over-simplification that is impossible to test the results empirically; it should then be useful to consider alternative approaches which analyse the consequences as interrelationships involving directly the empirical values of  $B_r$ ,  $H_{cI}$  and  $H_{cB}$ . However, it is then still necessary to assume that simple relations exist between these parameters of a particular magnet and the corresponding parameters of a second magnet, before the magnetic behaviour of the two can be compared with each other.

## 4.2. $X$ , $Y$ ratios and demagnetization quadrant form

Our early attempts to analyse magnetic data directly suggested that the assumption of simple relations between like parameters of two different magnets is not entirely satisfactory. In particular, it was observed that between magnets that are similar both with respect to material as well as aspects of fabrication processes, there is a clearer correlation when the coercivity values are scaled by the respective  $B_r$  values of these magnets [1, 2]. The resultant  $X$ ,  $Y$  ratios, when plotted, define a common curve for certain similar magnets which we then consider as constituting a set. Regression expressions fitted to each curve provide the equations relating the  $X$ ,  $Y$  values for the different members of the set. These observations are now seen as arising from certain geometrical scaling aspects of the demagnetization quadrant that are common to the magnets within any specific set. We consider here demagnetization quadrants that are idealized as being of two linear segments,  $0 \leq H \leq H_{cB}$  and  $H_{cB} \leq H \leq H_{cI}$ , where  $H$  is the applied demagnetizing field, ignoring its negative direction in opposition to  $B$ , as has been the case with the  $X$ ,  $Y$  ratios themselves [1, 2]. Examples of such graphs are shown in Fig. 8 for the cases of (a)  $Y = H_{cB} = H_{cI}$  (the limiting  $Y = X$  case, Table I), and (b–d) for which  $H_{cB} = 0.5, 0.65$  and  $0.8$ , respectively, for the  $\text{SmCo}_{x \sim 5}$  polymer bonded, M(F) set. In fact the figure shows a superposition of the  $X$  versus  $Y$  common curve ( $Y = 0.567X^{0.432}$ ) and a number of demagnetization quadrant graphs. Superposition is made possible, without loss of generality, by taking  $B_r$  as having unit value. In this way, the vertical axis can either represent  $Y$  or  $4\pi M$ , where  $M$  ( $= I$ ) is the magnetization which is numerically the difference between  $B$  and the demagnetizing field,  $H$ . Similarly, the horizontal axis can equally well represent  $X$  or the demagnetizing applied field,  $H$ . It is clear from this figure that all the  $0 \leq H \leq H_{cB}$  (low  $H$ ) segments of the demagnetization quadrants will originate at the  $Y = B_r = 1$  corner of the figure and terminate at the respective  $H = H_{cB}$  ( $= Y$ ) intersections on the  $Y = X$  (or  $4\pi M = H$ ) line. The respective  $H_{cB} \leq H \leq H_{cI}$  (high  $H$ ) segments terminate at the appropriate  $H = H_{cI}$  ( $= X$ ) intersections on the horizontal ( $H$ ) axis. From these consid-

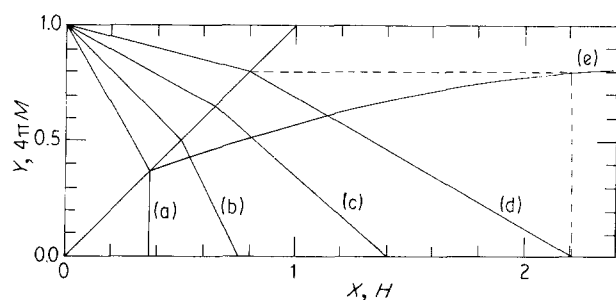


Figure 8 Demagnetization quadrants in terms of  $4\pi M$  versus  $H$ , and each as two linear segments for various examples associated with the M(F) magnet set: (a) for the limiting  $Y = X$  case where  $H_{cB} = H_{cI}$ ; (b–d) for the cases of  $H_{cB} = 0.5, 0.65$  and  $0.8$ , respectively. Broken lines show the relationship between the segments and the logarithmic curve for the magnet set, for  $H_{cB} = 0.8$ .

erations we see that it is not the individual segments that are specific to the magnets of a particular set but rather the characteristic matching of the segments that together form the demagnetization quadrant. This characteristic matching provides the geometrical reason for the common trajectory that is obtained when the empirical ( $X$ ,  $Y$ ) data of a particular magnet set are plotted.

In Fig. 9 the linearized demagnetization quadrants are shown in two pairs for the four identified type 2 sets. For the polymer bonded,  $\text{SmCo}_{x \sim 5}$ , pair of M(F) and HD(F), the example shown is that of  $H_{cB} = 0.8$  while  $H_{cI} = 0.95$  for the other pair of sintered PrSmCo(A) and NdDyFeB magnet sets. Despite the higher  $Y$  value, the projected  $H_{cI}$  (or  $X$ ) points for the latter pair fall between those of the polymer-bonded pair. Furthermore, as observed above, the type 2 logarithmic regression graphs are concurrent only at a point outside the physical  $Y = 1$  limit. Hence at any particular  $Y$  value the high  $H$  segments of the type 2 sets are always all distinct from each other. Finally, the  $H_{cI}$  (or  $X$ ) values for the polymer-bonded sets with  $Y = 0.95$  both far exceed those of the sintered sets, and are not shown in Fig. 9 as they lie outside the  $X$  range for the chosen  $X$  scale. The sintered pair of type 2 magnets always have significantly steeper high  $H$  segments than the polymer-bonded pair for the same low  $H$  segment because, as noted above, the logarithmic curves of the type 2 sets tend towards concurrency only for  $Y = 1.0695$ , which exceeds the physical limiting value of unity.

## 4.3. Magnetic domain pattern and flow analogue.

The nature of the particular ( $X$ ,  $Y$ ) trajectory has hitherto been applied to classify fabricated magnet sets into different types [3]. The present discussion suggests the subtly different aspect that the magnets in a particular set have a specific admixture of type 1 (represented by the low  $H$  segments) and type 2 (high  $H$  segments) demagnetization characteristics. Regression fit constants ( $K$ ,  $L$  for logarithmic regression and  $\alpha$ ,  $\beta$ , and  $\gamma$  for second-order polynomial regression) can then be obtained from empirical data to parametrize the demagnetization characteristics of a particular fabricated magnet set.

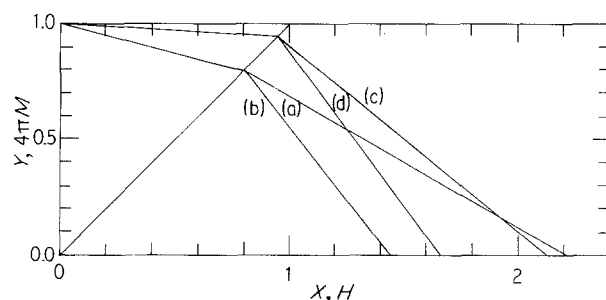


Figure 9 Demagnetization quadrants in terms of  $4\pi M$  versus  $H$ , and each as two linear segments for various examples associated with (a) the polymer-bonded M(F) and (b) HD(F) sets for the case  $H_{cB} = 0.8$  and with (c) the sintered PrSmCo(A) and (d) NdDyFeB sets for  $H_{cB} = 0.95$ .

Magnetic domain patterns that are associated with magnets that have type 1 demagnetization characteristics tend to be geometrically simple, mainly Euclidian polygonal, in section. With increasing type 2 demagnetization characteristics, the domain patterns become increasingly more complex, and suggest more of fractal geometry [17, 18]. This suggestion that type 1 and type 2 domain patterns are fundamentally geometrically distinct requires further investigation. For the present we shall only briefly consider certain aspects of this inference by comparison of the features from the logarithmic regression ( $Y = KX^L$ ) analysis of fabricated magnet sets with a fluid (Poiseuille) flow system analogue [19]. In particular, the domain pattern geometry of a fabricated cylindrical magnet that is being demagnetized in a field,  $H$  (ignoring a negative sign), is configured in an analogous way as an instantaneous flow pattern associated with Poiseuille flow in a cylindrical bore under an applied pressure head. The demagnetization of the magnet as  $H$  is varied alters the domain pattern, just as changes in the pressure head affect the flow pattern. Observed polygonal domain patterns that are associated with a linear  $Y = X$  relation and a low  $H$  regime are geometrically analogous to a laminar flow, which is a linear function of changing pressure head over a low-pressure range. Complex (fractal) domain patterns occur with increasing type 2 character which is manifested for a high  $H$  regime; analogously, increasingly turbulent flow is obtained with higher pressure head.

Just as laminar and turbulent flow (patterns) are analysed as distinct regimes in a fluid flow system, there is the analogy that the type 1 and type 2 magnetic domain patterns represent distinctive magnetic alignment geometries. Elucidation of the details of transition between the two regimes of flow constitutes a complicated and important branch of fluid dynamics in which the effects of a variety of physical disturbances of different scale are studied with respect to the manner in which they can induce the laminar-turbulent flow transition [19, 20]. Similarly, the present identification of the two distinctive magnetic domain pattern (type 1 and type 2) modes can allow an enhanced understanding of the different mechanisms that can trigger changes between these modes. In particular, discussion of domain nucleation and pinning mechanisms for demagnetization within a single magnet can be viewed afresh in terms of how they operate to account for the difference in the admixtures of type 1 and type 2 magnetic alignment modes between similar magnets which form a particular  $(X, Y)$  set, as well as between magnets associated with different  $(X, Y)$  sets.

## 5. Conclusion

Discrete point values such as  $B_r$ ,  $H_{cB}$  and  $H_{cI}$  cannot adequately fully parameterize the quasi-continuous demagnetization quadrant of the hysteresis loop for a ferromagnet. Consequently, even the comparison between the demagnetization behaviour of two magnets for which all the three values of one can never be

assumed to be exactly equal (not just in the sense of being measured to be empirically different but also in that numerically equal values can arise from different admixtures of fundamental magnetic alignment geometries), will be of limited usefulness. This deficiency suggests that the demagnetization characteristics of different magnets for which the ratios  $(X, Y)$  define a common trajectory can instead be usefully inter-compared on the basis of the equation(s) for the trajectory. Logarithmic and second-order polynomial regression analyses of the trajectories for empirical data that define 14 varied sets of fabricated ferromagnets suggest that there may be two basic modes of demagnetization for which the corresponding domain patterns are analogous to the two distinct laminar and turbulent flow patterns of a fluid flow system. Future work exploiting the possible analogy between demagnetization modes and fluid flow modes and their respective transition trigger mechanisms is envisaged.

## Acknowledgement

The author thanks Professor J. F. Knott, Head, School of Metallurgy and Materials, University of Birmingham, for an Honorary Research Fellowship during which term this paper was prepared with the facilities of the School.

## References

1. C. Y. TAY and I. R. HARRIS, *J. Mater. Sci. Lett.* **4** (1985) 114.
2. *Idem, ibid.* **5** (1986) 214.
3. C. Y. TAY, *J. Mater. Sci.* **23** (1988) 4517.
4. *Idem, J. Mater. Sci. Lett.* **10** (1991) 204.
5. *Idem, ibid.* **9** (1990) 1042.
6. M. TOKUNAGA, N. MEGURO, M. ENDOH, S. TANIGAWA and H. HARADA, *Trans. IEEE Magn. Mag.* **21** (1985) 1964.
7. D. LI, H. F. MILDRUM and K. J. STRNAT, *J. Appl. Phys.* **57** (1985) 4140.
8. D. L. MARTIN, M. G. BENZ and A. C. ROCKWOOD, in "AIP Conference Proceedings", Vol. 10, edited by C. D. Graham Jr and J. J. Rhyne (American Institute of Physics, New York, 1973) p. 583.
9. J. W. WALKIEWICZ and M. M. WONG, *Trans. IEEE Magn. Mag.* **15** (1979) 1757.
10. M. G. BENZ and D. L. MARTIN, *J. Appl. Phys.* **42** (1971) 2786.
11. F. G. JONES, M. DOSER and T. NEZU, *Trans. IEEE Magn. Mag.* **13** (1977) 1320.
12. R. C. CARRIKER, in "AIP Conference Proceedings", Vol. 10, edited by C. D. Graham Jr and J. J. Rhyne (American Institute of Physics, New York, 1973) p. 633.
13. J. T. SANDEFUR, "Discrete Dynamical Systems" (Oxford University Press, Oxford, 1990).
14. J. J. BECKER, *Trans. IEEE Magn. Mag.* **4** (1968) 239.
15. R. M. MAY, *Nature* **26** (1976) 459.
16. K. KUMAR, *J. Appl. Phys.* **63** (1988) R13.
17. B. B. MANDELBROT, "The Fractal Geometry of Nature" (Freeman, San Francisco, 1983).
18. B. H. KAYE, "A Random Walk through Fractal Dimensions" (VCH, New York, 1989).
19. D. J. TRITTON, "Physical Fluid Dynamics" (Oxford University Press, Oxford, 1988).
20. D. D. JOSEPH, "Stability of Fluid Motions", Vols 1 and 2 (Springer, Berlin, 1976).

Received 16 January 1991  
and accepted 19 May 1992